ISSN 2712-8008
Volume / Том 24 №4 2024
Journal Homepage: http://vestnik.pstu.ru/geo/

Perm Journal of Petroleum and Mining Engineering

UDC 622.245.14
Article / Статья

Application of Geomechanical Modeling Methods to Assess Casing Stability during Cumulative Perforation

Sergey E. Chernyshov[1], Sergey N. Popov[2], Xiaopu Wang[3], Hailong Zhao[3], Vadim V. Derendyaev[1], Aleksandr A. Melekhin[1]

[1]Perm National Research Polytechnic University (29 Komsomolskiy av., Perm, 614990, Russian Federation)
[2]Oil and Gas Research Institute of the Russian Academy Sciences (3 Gubkina st., Moscow, 119333, Russian Federation)
[3]National Key Laboratory of Deep Oil and Gas, China University of Petroleum (East China, Qingdao, China)
[4]School of Petroleum Engineering, China University of Petroleum (East China, Qingdao, China)

Применение методов геомеханического моделирования для оценки устойчивости обсадной колонны при кумулятивной перфорации

С.Е. Чернышов[1], С.Н. Попов[2], Сяопу Ванг[3,4], Хайлун Чжао[3,4], В.В. Дерендяев[1], А.А. Мелехин[1]

[1]Пермский национальный исследовательский политехнический университет (Российская Федерация, 614990, г. Пермь, Комсомольский пр., 29)
[2]Институт проблем нефти и газа РАН (Российская Федерация, 119333, г. Москва, ул. Губкина, 3)
[3]Национальная ключевая лаборатория глубоководной добычи нефти и газа, Китайский нефтяной университет (Китайская народная республика, г. Циндао, Восточный Китай)
[4]Школа нефтяной инженерии Китайского нефтяного университета (Китайская народная республика, г. Циндао, Восточный Китай)

Received / Получена: 24.04.2024. Accepted / Принята: 30.09.2024. Published / Опубликована: 31.10.2024

Keywords:
secondary opening, productive formation, well casing integrity, numerical finite element model, borehole zone, cement stone, well casing loads, cumulative perforation.

The stability analysis of the lining for two oil producing wells during secondary opening of productive formations using the cumulative perforation method was performed. The research was carried out using data from direct measurements of wellbore pressures at different distances from the cable tip of the perforating device at the time of detonation, which exceeded 50 MPa. The pressure values were approximated along the wellbore using a power dependence. For a reliable forecast of the stress-strain state of the near-wellbore zone of the perforation interval, the ANSYS finite element modeling software package was used. To determine the stress field, an axisymmetric finite element calculation scheme was built; the height of the model along the wellbore was 39 m. When modeling, it was taken into account that the geological and physical characteristics of the modeled formations differed in the depth of occurrence and the value of the formation pressure. The elastic-strength properties of the formed cement stone were determined in the course of laboratory experiments for various formulations of cement slurries. Based on the modeling results, the destruction areas and the strength margin of the cement stone were determined, as well as the values of radial displacements of the production string in the perforation interval. The developed model of the borehole zone and methodological approaches can be used in the future when choosing the optimal elastic-strength properties of the cement stone, perforation devices and technological parameters of perforation-explosive operations.

Ключевые слова:
вторичное вскрытие, продуктивный пласт, сохранность крепи скважин, численная конечно-элементная модель, околоскважинная зона, тампонажный камень, нагрузки на крепь скважин, кумулятивная перфорация.

Выполнен анализ устойчивости крепи для двух нефтедобывающих скважин при вторичном вскрытии продуктивных пластов методом кумулятивной перфорации. При проведении исследований использованы данные прямых замеров величин давлений в скважине на разном удалении от кабельного наконечника перфорационного устройства в момент детонации, которые превышали 50 МПа. Значения давлений аппроксимировались вдоль ствола скважины с помощью степенной зависимости. Для достоверного прогноза напряженно-деформированного состояния околоскважинной зоны интервала перфорации применялся программный комплекс конечно-элементного моделирования ANSYS. Для определения поля напряжений строилась осесимметричная конечно-элементная расчетная схема, высота модели вдоль ствола скважины составила 39 м. При моделировании учитывалось, что геолого-физические характеристики моделируемых пластов отличались глубиной залегания и величиной пластового давления. Упругопрочностные свойства формируемого тампонажного камня были определены в ходе лабораторных экспериментов для различных рецептур тампонажных растворов. По результатам моделирования определены области разрушения и запас прочности тампонажного камня, а также величины радиальных перемещений эксплуатационной колонны в интервале перфорации. Разработанные модель околоскважинной зоны и методические подходы могут быть использованы в дальнейшем при выборе оптимальных упруго-прочностных свойств тампонажного камня, перфорационных устройств и технологических параметров прострелочно-взрывных работ.

© **Sergey E. Chernyshov** (Author ID in Scopus: 57204938259, ORCID: 0000-0002-2034-3014) – Doctor in Engineering, Associate Professor, Head of the Department of Oil and Gas Technologies (tel.: +007 (342) 219 82 92, e-mail: nirgnf@bk.ru). The contact person for correspondence.
© **Sergey N. Popov** (Author ID in Scopus: 56440323800, ORCID: 0000-0002-1110-7802) – Doctor in Engineering, Chief Researcher, Head of Laboratory of oil and gas mechanics and formation physicochemistry (e-mail: popov@ipng.ru).
© **Xiaopu Wang** (Author ID in Scopus: 56542940600, ORCID: 0000-0003-1013-2691) – Doctor in Engineering, Associate Professor at the National Key Laboratory of Deep Oil and Gas (e-mail: wxp@upc.edu.cn).
© **Hailong Zhao** (Author ID in Scopus: 57208787593) – Doctor in Engineering, Experimenter at the National Key Laboratory of Deep Oil and Gas (e-mail: zhl@upc.edu.cn).
© **Vadim V. Derendyaev** (Author ID in Scopus: 58496503900, ORCID: 0000-0001-5506-2178) – PhD student, Assistant at the Department of Oil and Gas Technologies (tel.: +007 (342) 219 88 06, e-mail: v.v.derendyaev@mail.ru).
© **Aleksandr A. Melekhin** (Author ID in Scopus: 55531747500, ORCID: 0000-0002-0737-1360) – PhD in Engineering, Associate Professor at the Department of Oil and Gas Technologies (tel.: +007 (342) 219 82 07, e-mail: melehin.sasha@mail.ru).

© **Чернышов Сергей Евгеньевич** – заведующий кафедрой, доктор технических наук, доцент, лауреат премии Пермского края в области наук о Земле I степени (тел.: +007 (342) 219 82 92, e-mail: nirgnf@bk.ru). Контактное лицо для переписки.
© **Попов Сергей Николаевич** – заведующий лабораторией, главный научный сотрудник, доктор технических наук (тел.: +007 (499) 135 73 71, e-mail: popov@ipng.ru).
© **Ксяопу Ванг** – доцент, доктор технических наук (e-mail: wxp@upc.edu.cn).
© **Хайлун Чжао** – экспериментатор, доктор технических наук (e-mail: zhl@upc.edu.cn).
© **Дерендяев Вадим Валерьевич** – ассистент, аспирант (тел.: +007 (342) 219 88 06, e-mail: v.v.derendyaev@mail.ru).
© **Мелехин Александр Александрович** – доцент, кандидат технических наук (тел.: +007 (342) 219 82 07, e-mail: melehin.sasha@mail.ru).

Please cite this article in English as:
Chernyshov S.E., Popov S.N., Wang Xiaopu, Zhao Hailong, Derendyaev V.V., Melekhin A.A.Application of geomechanical modeling methods to assess casing stability during cumulative perforation. *Perm Journal of Petroleum and Mining Engineering*, 2024, vol.24, no.4, pp.194-203. DOI: 10.15593/2712-8008/2024.4.3

Просьба ссылаться на эту статью в русскоязычных источниках следующим образом:
Применение методов геомеханического моделирования для оценки устойчивости обсадной колонны при кумулятивной перфорации / С.Е. Чернышов, С.Н. Попов, Сяопу Ванг, Хайлун Чжао, В.В. Дерендяев, А.А. Мелехин // Недропользование. – 2024. – Т.24, №4. – С.194–203. DOI: 10.15593/2712-8008/2024.4.3

Introduction

The issue of behind-the-casing flows in production wells remains relevant despite numerous studies and developments aimed at creating durable, leak-proof well linings [1–3]. Often, the successful introduction of new cementing materials [4] and other process fluids [5–7] increases the share of continuous contact between the cement stone and adjacent environments. However, during various operations, the integrity of the cement ring behind the casing is not maintained. High loads on the well lining during secondary reservoir openings with cumulative perforators, hydraulic fracturing of productive formations, acid treatments, drilling out casing accessories and other types of work lead to the destruction of brittle cement stone and condition behind-the-casing flows [3, 8]. As shown in the works [9–11], high pressures in the well can also occure during the formation of hydraulic fractures, which negatively influences the well cement lining integrity [12, 13].

To prevent early well production flooding and extend the period of water-free operation, it is necessary to assess the stability of the formed cement stone, considering its physical and mechanical properties, the maximum excess pressure on the linings and other factors [8, 14–17].

In researches devoted to cumulative perforation, the issue of cement stone integrity has been studied insufficiently. In the article [18], the authors consider the effect of perforation channels failure in cement stone taking into account their eccentricity. However, the researchers do not account for the stress distribution in the production casing and the surrounding rock mass. Similar assumptions are made in the work [19], where the authors determine the stress values on the walls of perforation channels in directional wells using analytical dependencies.

In the research [20], the influence of the cumulative charge is shown only on the porosity and permeability of the reservoir rock. In the work [21], the authors optimize the formation of perforation channels in multi-layer coal seams for methane production. In the article [22], propagation of fractures during multi-stage hydraulic fracturing in horizontal wells is considered, taking into account the perforation channels.

In most cases, maximum excess pressures on the well lining occur during secondary opening of productive formations using the cumulative perforation method [3, 23–25]. The pressure values depend on many factors, such as the type of perforating charge, perforation density, perforation interval depth, well geometric parameters, and others.

It is possible to solve the problem of assessing the cement stone integrity when performing various technological operations by development of a well lining model and determining the actual values of the elastic-strength characteristics of the cement material, as well as measuring excess pressures in the well. The approach will allow us to identify a potential lining seal failure, as well as to determine the maximum permissible loads on the well lining. Furthermore, it will establish requirements for the physical and mechanical properties of the cement stone, as well as develop recommendations for the technological parameters of cumulative perforation. Additionally, it will enable to assess the efficiency of various methods to reduce the risks, considering specific conditions of work on the secondary opening of productive formations.

The excess pressures effect on the well lining is closely connected with the methodological techniques of blasting-perforation operations (BPO) during secondary opening of formations. It is mainly associated with the type of cumulative charges (perforation systems) and the perforation density for specific geological and technical conditions of its operation. The excess pressures are defined as the difference between the maximum measured value and the hydrostatic pressure formed by the fluid column in the well:

$$P_{\text{exc.}} = P_{\text{max}} - P_{\text{hydr}}, \quad (1)$$

where $P_{\text{exc.}}$, P_{max}., и P_{hydr}. are the values of excess, maximum, and hydrostatic pressures, respectively. In this case, the casing is affected by the maximum measured pressures.

Along with the development and application of cement compositions having optimal elastic-strength properties to ensure the integrity of cement stone during blasting-perforation operations, special equipment and technologies should be used to reduce excess pressures [15, 26, 27]. Modern analogs of pressure compensators, as mechanical implosion devices (chambers) are used to reduce excess pressures and to create a dynamic depression for cleaning perforation channels, which is considered as their major purpose. Implosive chambers that use technological charges for their decompression, such as the "ΔP technology" and "PURE," can lead to an additional increase in pressure [28].

Less expensive methods of reducing pressures may be selective perforation technologies with a decrease in perforation density during the initial shot. It can be implemented by a time delay in the operation of each perforator in the assembly, with the first perforation carried out in the most porous (permeable) section of the productive formation. The section will then act as a compensator, neutralizing the explosive effect on the well lining. The simplest method modification is the secondary opening of the mentioned formation section with a reduced charge density (5–10 holes) by a separate perforator run. An even more effective modification is preliminary drilling of several holes with drilling perforators.

Manufacturers of perforating systems are also working on improvements aimed at preserving cement stone behind the casing during blasting-perforation operations. For example, specialists of Promperforator LLC have developed a methodology for perforation with paired grouping of charges. In the perforators, cumulative charges are divided into groups of one or more pairs of charges. According to the field tests, the explosive impact inside the perforator was reduced by at least 20 %, the explosive load on the well lining was halved, the reservoir drainage coverage and the feeding zone of each perforation channel were increased [29].

Research on the theoretical and experimental reasoning of the secondary perforation quality has not

Table 1

Dynamics of excess pressure changes at a distance from the perforator up to 100 m

Field, well	Charges			Perforation interval, m	Reservoir properties, K_{por}/K_{clay}	Pressure, MPa	
	type	mass of explosive, g	number of holes (total explosives, g)			P_{max} (distance from blasting-perforation device)	P_{exc}
Tanypskoe, A	ZPKT 105 *N-TV-SP1*; ZPKT 105 *N-TV-OP1*	33.3	20 + 20 (1333)	1599.0–1601.0	8/17	54.3 (1 m)	38.8
						33.8 (50 m)	18.8
						31.6 (100 m)	17.1
Tanypskoe, B	ZPK 102AT-M-03; ZPK 102AT-M-10	28.0; 27.5	20 + 20 (1110)	1563.0–1565.0	25/5	50.0 (1 m)	33.7
						50.3 (5 m)	34.0
						44.6 (20 m)	28.5
						31.6 (40 m)	15.7
Mokhovskoye, C	ZPK 102 AT-M-03	28.0	40 (1120)	1648.5–1650.5	10–19/7–50	38.1	21.0
			60 (1680)	1627.0–1630.0	11–20/8–30	40.9	23.9
			40 (1120)	1624.0–1626.0	11–18/6–27	39.8 (2 m)	22.8
						38.8 (3 m)	21.8

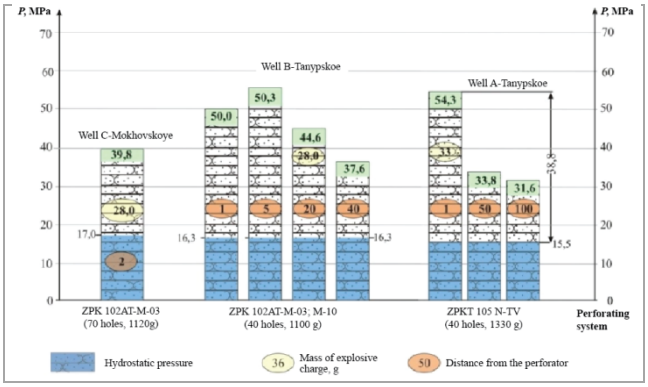

Fig. 1. Pressure measurement results during cumulative perforation

been conducted for a long time, and the well-known fundamental recommendations were developed back in the last century [30]. Within the traditional approach, the perforation density typically 20 and 30 holes per meter for terrigenous and carbonate reservoirs, respectively, does not consider the bottom-hole and formation pressures (depression, repression), the composition of perforating fluids, and the reservoir properties. Additionally, the physical processes occurring in the rock and cement stone due to the impact of short-term reversal load during the perforator operation are not considered either. The influence degree on the well lining from blasting-perforation operations (BPO) is also not regulated in the state standard for cumulative charges (GOST 55777-2013) [31]. The document states that the charges should provide minimal impact on the well structure integrity during standard perforator operation. At the same time, it is noted that the explosive mass (EM) should ensure maximum penetration parameters while having minimal impact on the well lining.

Measuring well pressure

At the initial stage of the research, measurements of actual excess pressure values were carried out during blasting-perforation operations using various modifications of perforating-explosive equipment (PEE). The measurements were conducted using independent devices placed in close proximity to the perforator and the interior pressure gauge located at distances up to 100 m from the productive interval. To provide detailed measurements in the nearest area to the perforator, where the highest pressure values are observed, the instruments were attached to a geophysical cable at distances of 1–3, 5, 10, 20, 25, and 40 meters from the cable head, while simultaneous measurements were performed with 3 to 4 instruments. The autonomous devices included modified electronic instruments AMT-10UM and ACM-8, with sampling interval of 0.067 and 0.25 ms, respectively (15,000 and 4,000 samples per second).

At distances of 5 meters or more from the perforator, interior pressure gauges were installed, each containing two instruments (columns). The wellbore fluid pressure was transmitted through the pistons of the instruments to the crushing columns located in a sealed cavity, deforming their conical part. As a result of measurements with a micrometer on the crushed part's length, the maximum force at which the column deformed was determined using the calibration table, as well as the maximum pressure occurring in the wellbore during cumulative perforation.

In total, over 100 measurements of maximum pressures were performed during secondary opening of terrigenous and carbonate reservoirs with various types of perforators, using electronic and interior pressure gauges, from which their excess values were calculated (Fig. 1). The results did not establish a direct correlation between the excess pressure $P_{exc.}$ and the mass of explosives, which is directly related to the number of perforated holes. A considerable variation in their values is noted across different types of charges and perforating systems of various modifications. Regarding the dynamics of pressure changes relative to the distance from the perforator, it was observed that the excess pressure values decrease systematically with increasing distance from the cable head of the perforating-explosive equipment. Moreover, in the overwhelming majority of wells, the pressures $P_{exc.}$ at a distance of 50 m from the perforator decrease by two times or more [23].

As an example, Table 1 presents the measurements and calculations of maximum and excess pressures in wells A and B of the Tanypskoye and C of the Mokhovskoye fields, where terrigenous deposits of the Visean stage (C1v) with varying values of reservoir properties were perforated. In well A, the reservoir had the porosity and clay content (K_{por} and K_{clay}) of 8 % and 17 %, respectively. In other wells, as can be seen from Table 1, these parameters are a bit higher. Table 1, as well as Fig. 1, show that in wells A and B, where high values of excess pressure were recorded, reaching 38.8 and 33.7 MPa at 1 m from the

perforator, they decreased by more than two times at 50 and 40 m above the perforator, respectively.

Their values were 18.8 and 15.7 MPa, which corresponds to a reduction of 52 % and 53 % compared to readings from the instruments installed near the perforating-explosive equipment. At a distance of 100 m from the cable head, the additional decrease in P_{exc} is insignificant and in the well A it was only 1.7 MPa in relation to the measurement by the instrument located at 50 m closer to the perforating-explosive equipment.

Considering the dynamics of pressure changes in Well B, it should be noted that the interior pressure gauge installed at a distance of 5 m from the cable head or 4 m from its electronic analogue, registered the highest pressure of 50.3 MPa. According to the measurements taken at 1 m from the perforator with an autonomous device, the pressure was recorded at 50.0 MPa. The reason for the lower readings of electronic devices, in comparison with pressure gauge, lies in the discrete method of their measurements.

As an example, let us consider the dynamics of pressure changes in well C of the Mokhovskoye field during secondary opening of the interval 1624.0–1626.0 m (Fig. 2). The maximum value measured by the autonomous device ACM-8 at 2 m from the cable head is 39.8 MPa, while the value recorded by the AMT-10UM at 3 m is 38.8 MPa. From Fig. 2 it is evident that after the perforator is initiated, within less than 0.2 ms there is a sharp increase in pressure less than 0.2 milliseconds, reaching 34.2 MPa (AMT-10UM). Then, after the gases breakthrough into the internal cavity of the perforator, its sharp drop to 25.0 MPa occurs. The positive extreme of 38.8 MPa is reached by the pressure after 2.4 ms, after which it decreases. However, the extreme does not reflect the actual value of $P_{max.}$. The maximum pressure value is between two adjacent points (samples) with the highest values, recorded approximately at 2.3 and 2.4 ms. It is also worth noting that the discrepancies in the pressure values registered by the AMT and ACM devices are explained by their different distances to the perforator and different sampling times.

Thus, the assessment of the expected maximum pressure values recorded by autonomous devices does not exclude possible errors in their determination. In cases where the sampling time coincides with the extreme corresponding to the maximum pressure value, the device will register it. However, the probability of such a coincidence is low due to the relatively large discretization step in measuring alternating pressures arising during perforation. It does not allow the obtained results to be used for an accurate assessment of their absolute values during the initial period of perforation effect on the lining.To increase the accuracy, it is necessary to develop and use devices with a higher sampling frequency or to rely on interior pressure gauge.

In modeling the cement stone stability and the production string under conditions of formation opening by cumulative perforation, real pressure measurements from wells C-Mokhovskaya and A-Tanypskaya were used during the geological and technological operations (GTO). The pressure values were approximated along the wellbore using a power dependence (Fig. 3).

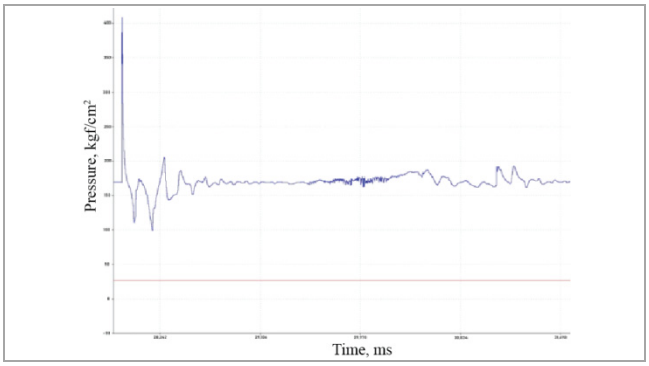

Fig. 2. Dynamics of pressure changes measured by electronic gauges during perforation in well C

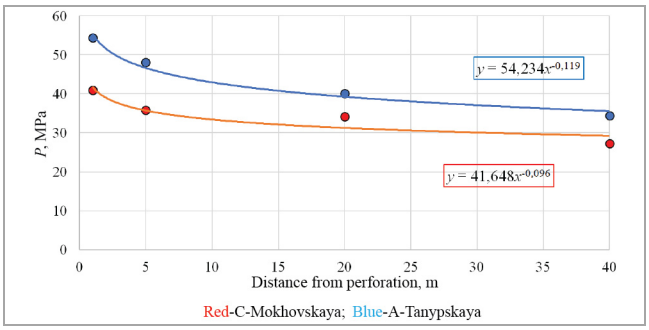

Fig. 3. Distribution of measured pressure in wells C-Mokhovskaya and A-Tanypskaya during cumulative perforation and its approximation

Numerical modeling

For a reliable forecast of the wellbore zone stress-strain state (SSS), the finite element method has become the most widely used [32, 33]. The method allows for determining the stress distribution field in the elements of well structures and the surrounding rock mass, both with constant model properties and in case of their transformation under the influence of various factors, such as corrosion, wall collapse, poor cementing, and others [34–36].

Numerical calculations and analysis of wellbore zone stress-strain state were performed using the ANSYS finite element modeling software package. The software product has proven to be quite effective in solving problems related to oil and gas geomechanics [8, 33, 37]. It was assumed that the deformations of the casing, cement and rock follow Hooke's law of linear elasticity. The ANSYS software package implements the fundamental relationships describing the behavior of elastic materials, which are detailed in works [38, 39].

In the numerical method for calculating stresses near a well, three types of equations are used:

– equations of motion (moments):

$$\sum_j \frac{\partial \sigma_{ij}}{\partial x_j} + \rho f_i = 0;\ i, j = 1, 2, 3, \qquad (2)$$

where σ_{ji} – stress tensor components; ∂x_j – derivative with respect to the j coordinate; ρf_i – mass forces;

– geometric relationships:

$$\varepsilon_{ij} = \frac{1}{2}\left(\frac{\partial u_i}{\partial x_j} + \frac{\partial u_j}{\partial x_i}\right);\ i, j = 1, 2, 3, \qquad (3)$$

where ε_{ji} – components of the strain tensor; u – components of the displacement vector;

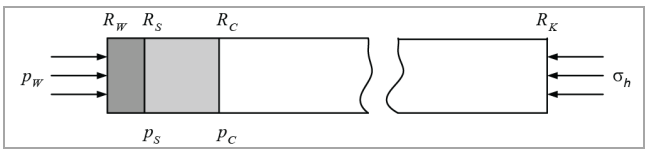

Fig. 4. Cased well diagram: p_s – pressure at the point of contact between the well casing and the cement lining; R_S – inner radius of cement lining

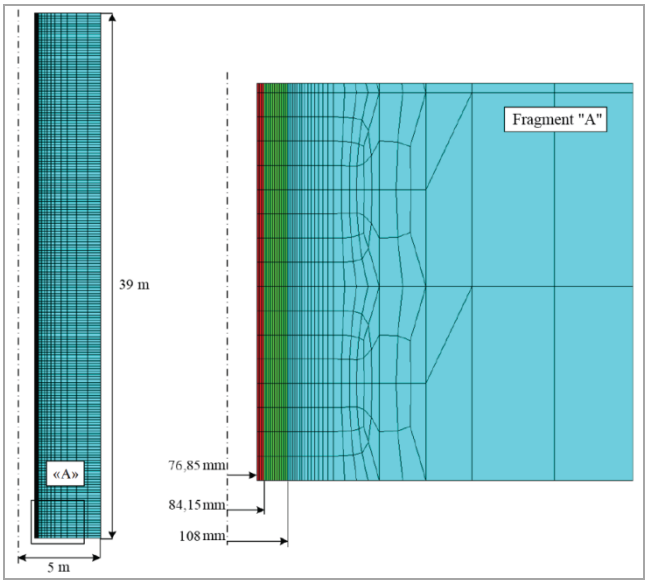

Fig. 5. Finite element diagram of the near-wellbore zone, used in calculations (red – casing column, green – cement stone, blue - reservoir rock)

Table 2

Geometric characteristics of the model and elastic strength properties of the column

Characteristics	Value
Column outside diameter, mm	168.3
Column thickness, mm	7.3
Drilling tool diameter, mm	215.9
Model radius, m	5.0
Young's modulus of the column, GPa	200.0
Poisson's ratio of the column, fraction units	0.2
Yield strength of column steel, MPa	372.0

– physical relationships (in this case, Hooke's law of linear elasticity):

$$\{\sigma\} = [D]\{\varepsilon\}, \quad (4)$$

where $\{\sigma\}$ – stress vector; $[D]$ – matrix of elastic constants; $\{\varepsilon\}$ – strain vector.

When using the finite element method, the above equations are transformed into a system of linear equations, which is solved with the unknown displacement vector:

$$[K]\{u\} = \{F\}, \quad (5)$$

where $[K]$ – the global stiffness matrix of the system; $\{u\}$ – the nodal displacements vector of the model; $\{F\}$ – the vector of external forces.

Then, based on the calculated displacement vector, stresses and strains are determined from expressions (2) and (3).

We developed an axisymmetric finite element calculation scheme to determine stresses in the wellbore zone (Fig. 4, 5).

To assess the integrity of the cement stone in the first approximation, a quasi-static problem was solved using the pressure curves of the fluid in the well, determined during experiments. Since the elastic porous medium deformation under the shock wave effect occurs over a very short period of time, the undrained loading conditions were applied. In this case, the stresses near a vertical well are expressed by well-known equations for unsaturated rocks (using undrained elastic constants):

$$\sigma_r = \sigma_h - (\sigma_h - p_w)\frac{R_w^2}{r^2}; \quad \sigma_\Theta = \sigma_h + (\sigma_h - p_w)\frac{R_w^2}{r^2}; \quad (6)$$

where σ_h – lateral rock pressure; p_w – bottomhole pressure; r – current radius; R_W – outer radius; σ_Θ – shear stress; σ_r – radial stress.

Equations (6) are applicable to open wells. For cased wells, these equations are valid in the range from R_C (the outer radius of the cement lining) to R_K (the radius of the feeding contour). In this case, the bottomhole pressure p_W in the well is performed by the pressure at the cement-rock contact p_C (see Fig. 4).

The stresses in the casing and cement sheath are calculated using Lame's formulas for a thin-walled cylinder [8]:

$$\sigma_{\Theta,1} = \frac{2R_2^2 p_2 - p_1(R_1^2 + R_2^2)}{R_2^2 - R_1^2}; \quad \sigma_{\Theta,2} = \frac{p_2(R_1^2 + R_2^2) - 2R_1^2 p_1}{R_2^2 - R_1^2}, \quad (7)$$

where $\sigma_{\Theta,1}$, $\sigma_{\Theta,2}$ – shear stresses on the inner and outer contours of the cylinder; R_1, R_2 – inner and outer radii of the cylinder; p_1, p_2 – pressure in the inner and outer contours.

Pressures p_1 and p_2 are the bottomhole pressure p_w and the pressures at the contacts p_c and p_s (the pressure at the contact of the casing with the cement). To calculate the contact pressures p_s и r_s, the condition of displacement continuity at the contact points is used. For example, for the casing contact with the cement, the condition of displacement continuity is expressed as follows [8]:

$$u = \frac{R_s}{E_s}\left[(1-\nu_s^2)\sigma_\Theta - \nu_s(1+\nu_s)p_s\right] = \frac{R_s}{E_c}\left[(1-\nu_c^2)\sigma_\Theta - \nu_c(1+\nu_c)p_c\right], \quad (8)$$

where R_W, R_S, R_C – the inner and outer radii of the casing and the nominal radius of the open hole; E_S, ν_S – modulus of elasticity and Poisson's ratio of the casing; E_C, ν_c – modulus of elasticity and Poisson's ratio of cement stone.

The calculations used typical column characteristics applied for oil fields in Perm Krai. It was assumed that the well is directed vertically and consists of a production casing, cement lining and a section of reservoir rocks. The model height along the wellbore was 39 m corresponding to the sections of measured

pressures (see Figs. 3, 4, 5). The geometric characteristics of the model and the elastic strength properties of the casing are presented in Table 2.

Materials properties

The geological and physical properties of the simulated reservoirs differed in the depth of occurrence and the magnitude of reservoir pressure in particular (Table 3). Table 3 presents the characteristics of the elastic reservoir used in the calculations.

When constructing the model, it was assumed that two formulations of cementing the production casing could be used in the productive formation interval: a modified cementing composition with an expansion additive (composition No. 3) and one without it (composition No. 1), both with a density of 1.85 g/cm^3 based on Portland cement of grade PCT-I-G. Additionally, for comparison, an additive-free cementing composition with a density of 1.85 g/cm^3 based on Portland cement of grade PCT-I-G was prepared (composition No. 2).

To determine the physical and mechanical properties of the cement stone, samples with a diameter of 30 mm and a height of 60 mm were prepared, and their uniaxial compression tests were conducted according to State Standard [40, 41].

The uniaxial tensile strength was determined by splitting method on cylindrical samples according to State Standard [40]. The prepared samples were stored at room temperature to gain strength for 7 days. The strength limit for the Brazilian test was calculated according to ASTM-3967-16 (Fig. 6, *b*).

The elastic strength properties of the formed cement stone were determined during laboratory experiments based on regulatory documents; their average values are presented in Table 4.

As can be seen from Table 4, the physical and mechanical properties of the various compositions differ significantly, especially the compressive strength, which should influence the possible areas of cement stone failure under the same load values.

The following boundary conditions were used in the model:

– fixing the movements of the lower and upper boundaries along the vertical axis;

– on the right boundary, the value of horizontal stresses was set with the principle of effective stresses;

– on the left boundary (the inner wall of the column) the pressure distribution was applied according to the dependencies shown in Fig. 3.

Results

Using the constructed finite element model, a multivariant numerical simulation of the stress-strain state in the near-wellbore zone during the cumulative perforation was carried out. To analyze the column stability, the maximum stress was compared with the yield strength of steel (see Table 2). When studying the stresses in the cement lining, the linear dependence of the Coulomb-Mohr failure criterion was used.

The main results of the calculations are presented in Figs. 7–9. Fig. 7 shows the zones of failure in the cement stone obtained for the two examined wells using three types of cement. The data from Fig. 7

Table 3

Characteristics of productive formations used in calculations

Characteristics	Field, formation	
	Sh-Gozhanskoe, Tl, BB	Tanypskoe, Tl
Young's modulus, GPa	30	
Poisson's ratio, fraction units	0.25	
Biot coefficient of the rock, fraction units	0.85	
Average depth of perforation interval, m	1640	1600
Reservoir pressure, MPa	17	15

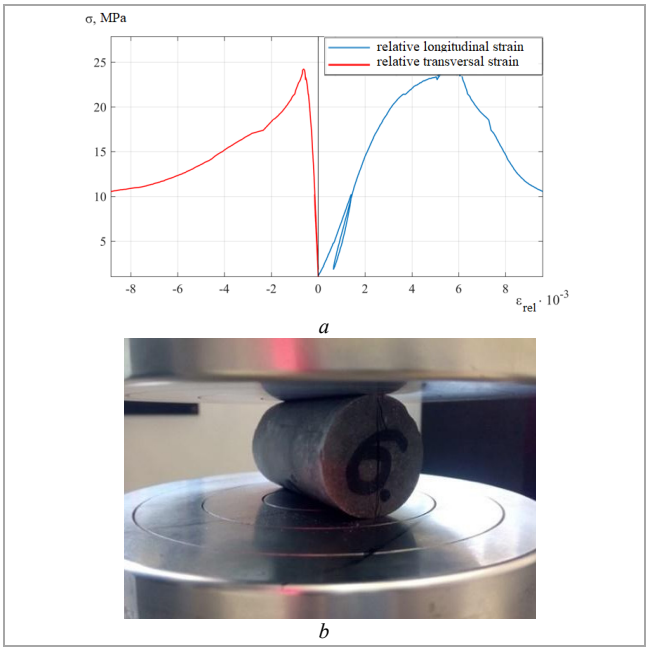

Fig. 6. Cement stone strength determination for uniaxial compression (formula 2) (*a*); Brazilian test (*b*)

Table 4

Elastic strength characteristics of plugging materials

Characteristics	Number of the plugging materials composition		
	1	2	3
Young's modulus, GPa	11.3	8.6	8.8
Poisson's ratio, fraction units	0.179	0.139	0.143
Compressive strength limit, MPa	31.5	24.4	13.7
Tensile strength limit, MPa	4.08	3.46	3.49
Angle of internal friction,°	29.6	28.6	22.3

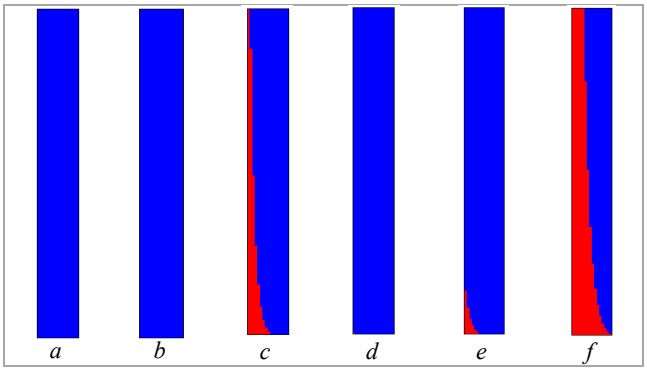

Fig. 7. Distribution of cement stone failure areas (in red) at perforation in C-Mokhovskaya (*a, b, c*) and A-Tanypskaya (*d, e, f*) wells under well lining conditions with plugging material of composition No. 1 (*a, d*), No. 2 (*b, e*) and No. 3 (*c, f*) (horizontal to vertical scale ratio 1:200)

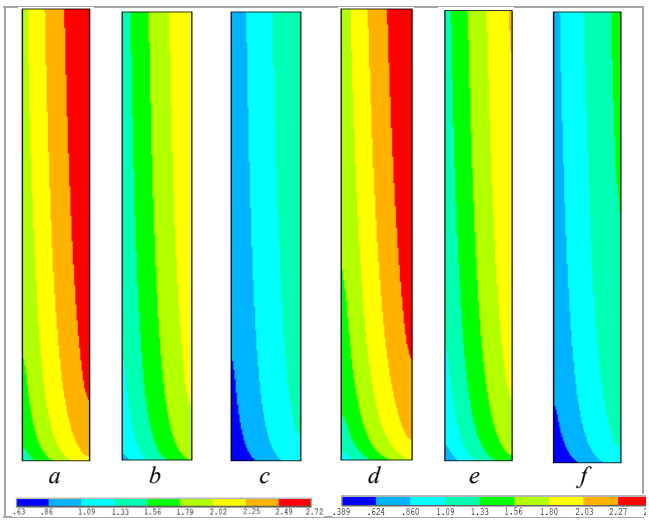

Fig.8. Safety factor distribution of cement stone in wells No. C-Mokhovskaya (*a, b, c*) and No. A-Tanypskaya (*d, e, f*) under well lining conditions with plugging material of composition No. 1 (*a, d*), No. 2 (*b, e*) and No. 3 (*c, f*) (horizontal to the vertical scale ratio 1:200)

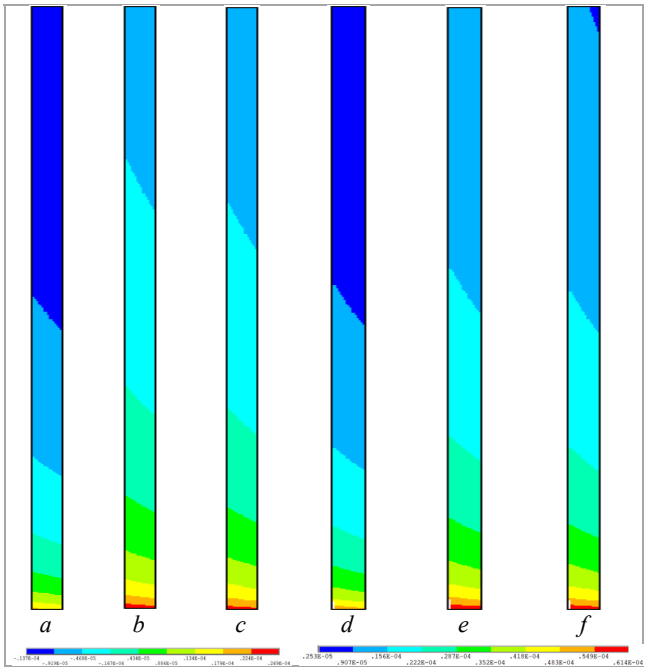

Fig. 9.Distribution of radial displacements (m) in the production casing of wells C-Mokhovskaya (*a, b, c*) and A-Tanypskaya (*d, e, f*) under well casing conditions with plugging material of composition No. 1 (*a, d*), No. 2 (*b, e*) and No. 3 (*c, f*) (horizontal to vertical scale ratio 1:200)

indicate that the largest failure zones occur for the composition of cement material No. 3 (see Fig. 7 *c, f*) for both wells C and A. This fact is consistent as composition No. 3 has the poorest strength properties. At the same time, for well A, the failure zones are a bit larger, which is related to the highest pressure in the well during perforation. The greatest thickness of the failure zone is observed in the area of maximum pressures near the perforation. Away from the interval, the failure thickness decreases due to the pressure reduction in the well.

For plugging material No. 1 under the same conditions as for wells C and A, according to calculations, areas of destroyed cement stone should be absent, which is facilitated by good strength indicators of the cement composition (see Fig. 7, *a, d*). For composition No. 2, failure areas occur only in well A, which is also related to a higher pressure of the gas generated by the explosive (see Fig. 7, *e*).

The preservation coefficient of the cement stone was calculated using the following equation (9):

$$k = \frac{\sigma_c}{\sigma_e}, \quad (9)$$

where, σ_c – strength of the cement stone under uniaxial compression, MPa; σ_e – calculated effective stresses acting on the cement stone, MPa.

For a more detailed analysis, Fig. 8 shows the distribution of the safety coefficient in the cement lining. It is assumed that if the coefficient is greater than one, the material remains in an elastic (undamaged) state, otherwise the cement is destroyed. The results presented in Fig. 8 generally confirm the results shown in Fig. 7.

From the data in Fig. 8 it follows that cement composition No. 1 has the best safety coefficient and its maximum value reaches 2.72 for perforation conditions in well C, and 2.51 for well A. The lowest safety coefficient is observed for cement composition 3 and is 0.63 for well C and 0.389 for well A.

Overall, the calculations presented in Figs. 7 and 8 indicate that high pressures in wells, resulting from the explosion of cumulative charges, can lead to the destruction of cement lining. Therefore, while casing in the studied productive formations, the plugging compositions should be selected to withstand the technological loads, ensuring a safety margin. In particular, it is recommended to use cement composition No. 1.

Stress-strain analysis of the production column showed that in all simulated cases, the stress levels do not exceed the yield strength, indicating its high stability. Fig. 9 presents calculated radial displacements for the perforation conditions in wells C and A, using three different cement compositions. As observed from the data in Fig. 9, the maximum displacements do not exceed 0.061 mm, further confirming the column's stability under the calculated conditions.

Discussion

Thus, the results of numerical finite element modeling of stress-strain state in the near-wellbore zone under cumulative perforation conditions and considering three formulations of grouting mortar were obtained in the research, which allowed for the following main conclusions:

1. As part of the study, a numerical finite element model of the near-wellbore zone was developed, including the production casing, cement stone and a reservoir rock section. The model allows for the specification of the measured uneven pressure distribution inside the well during cumulative perforation, considering various elastic and strength properties of the cement stone.

2. The calculations showed that when using the plugging material with composition No. 3, extensive failure zones occur for wells C and A, which is associated with the low strength properties of the

cement composition. At the same time, for well A, the areas are larger due to the higher value of the recorded pressure in the well during perforation.

3. For cement formulation No. 1, having better strength properties, the calculated scenarios showed no zones of failure; thus, in practice, it is most preferable to use the formulation for well cementing. For composition No. 2, zones of cement failure occur only for well A, which is a consequence of the higher pressure during perforation in the well.

4. The distribution of the safety factor values confirms the identified zones of cement failure and indicates that cement composition No. 1 has the best safety factor, with a maximum value of 2.72 for the perforation conditions in well C and 2.51 for well A. The lowest safety factor is observed for cement formulation No. 3, which amounts to 0.63 for well C and 0.389 for well A, indicating that the cement lining in well A is more susceptible to the risk of collapse.

5. The column's stress-strain analysis showed that the structural element of the well is quite stable in the simulated conditions. The result is confirmed by the radial displacements values in the column, which in the worst-case scenario reach only 0.061 mm.

6. The numerical finite element model of the wellbore zone and methodological approaches developed within the research can be used in the future, to select the optimal elastic strength properties of cement stone, as well as for determining the characteristics of the cumulative charge used for perforation.

Conclusion

The research is devoted to solving the relevant and significant problem of ensuring the well lining integrity. Modern developments in materials and technologies for cementing the casing strings of oil and gas wells enable to make a reliable sealed lining. However, even at the secondary opening of productive reservoirs, the integrity of the lining can be compromised. It often results in cross flow behind casing and inter-formation flows, leading to early water breakthrough, which results in inefficient and costly repair works.

To assess the stability of the lining elements (the cement stone and casing pipes), measurements of the pressure values generated during blasting-explosive operations were taken, as well as studies to determine the physical and mechanical rock properties and the formed cement stone. These data were used in the development of a numerical finite element model of the wellbore zone in the perforation interval.

Based on the results of numerical finite element modeling of the stress-strain state for the wellbore zone in the studied interval during cumulative perforation, the failure areas and the safety margin of the cement stone were identified, along with the radial displacements values of the production casing in the perforation interval for two oil-producing wells. The methodological approaches can be applied to determine the optimal formulations of cementing compositions for lining in the productive part of the wellbore section, as well as for selecting the main technological perforation parameters.

References

1. Krylov D.A., Marabaev N.A., Talamanov E.N., Burkhailo V.A., Serenko I.A. Izmenenie kontakta tsementnogo kamnia s metallom obsadnykh trub pri razlichnykh mekhanicheskikh vozdeistviiakh [Changes in the contact of cement stone with the metal of casing pipes under various mechanical influences]. *Burenie*, 1981, no. 7, pp. 18-21.
2. Shishin K.A., Rustambekov T.F., Krylov D.A. Vliianie opressovki i perforatsii skvazhin na kachestvo razobshcheniia plastov [The influence of well pressure testing and perforation on the quality of layer separation]. *RNTS "Burenie"*, Moscow: VNIIOENG, 1977, iss. 4, pp. 25-27.
3. Chernyshov S.E., Ashikhmin S.G., Kashnikov Iu.A., Savich A.D., Mosin A.V., Chukhlov A.S. Otsenka sokhrannosti krepi skvazhin posle provedeniia kumuliativnoi perforatsii s uchetom kriteriia razrusheniia tsementnogo kamnia [Evaluation of the cement sheath safety after shaped charge perforation considering the criterion of cement stone destruction]. *Neftianoe khoziaistvo*, 2021, no. 6. pp. 50-53. DOI: 10.24887/0028-2448-2021-6-50-53
4. Kremieniewski M. Recipe of Lightweight Slurry with High Early Strength of the Resultant Cement Sheath. *Energies*, 2020, vol. 13, 1583 p. DOI: 10.3390/en13071583
5. Kremieniewski M. Hybrid Washer Fluid for Primary Cementing. *Energies*, 2021, vol. 14, 1295 p. DOI: 10.3390/en14051295
6. Kremieniewski M., Wiśniowski R., Stryczek S., Łopata P. Comparison of Efficient Ways of Mud Cake Removal from Casing Surface with Traditional and New Agents. *Energies*, 2021, vol. 14, 3653 p. DOI: 10.3390/en14123653
7. B Roque.A.C., Brasileiro P.P.F., Brandão Y.B., Casazza A.A., Converti A., Benachour M., Sarubbo L.A. Self-Healing Concrete: Concepts, Energy, Saving and Sustainability. *Energies*, 2023, vol. 16, 1650 p. DOI: 10.3390/en16041650
8. Ashikhmin S.G., Chernyshov S.E., Kashnikov Iu.A., Makdonald D.I.M. Vliianie orientatsii i skhemy razmeshcheniia kanalov shchelevoi perforatsii na pronitsaemost' terrigennykh kollektorov v okoloskvazhinnoi zone plastov [A geomechanical analysis of the influence of orientation and placement of jet slots on terrigenous reservoir permeability]. *Neftianoe khoziaistvo*, 2018, no. 6, pp. 132-135. DOI: 10.24887/0028-2448-2018-6-132-135
9. He J.C., Zhang K.S., Liu H.B., Tang M.R., Zheng X.L., Zhang G.Q. Laboratory investigation on hydraulic fracture propagation in sandstone-mudstone-shale layers. *Petroleum Science*, 2022, vol. 19, pp. 1664-1673. DOI: 10.1016/j.petsci.2022.03.018
10. Wang J., Xie H.P., Matthai S.K., Hu J.J., Li C.B. The role of natural fracture activation in hydraulic fracturing for deep unconventional geo-energy reservoir stimulation. *Petroleum Science*, 2022, vol. 19, pp. 1664-1673. DOI: 10.1016/j.petsci.2023.01.007
11. Xu H., Ma T., Peng N., Yang B. Influences of Fracturing Fluid Injection on Mechanical Integrity of Cement Sheath under Four Failure Modes. *Energies*, 2018, vol. 11, 3534 p. DOI: 10.3390/en11123534
12. Deng Q., Zhang H., Li J., Hou X., Zhao B. Numerical Investigation of Downhole Perforation Pressure for a Deepwater Well. *Energies*, 2019, vol. 12, 3795 p. DOI: 10.3390/en12193795
13. Deng Q., Zhang H., Li J., Hou X., Wang H. Study of Downhole Shock Loads for Ultra-Deep Well Perforation and Optimization Measures. *Energies*, 2019, vol. 12, 2743 p. DOI: 10.3390/en12142743
14. Chernyshov S.E., Kunitskikh A.A., Votinov M.V. Issledovanie dinamiki gidratatsii i razrabotka sostavov rasshiriaiushchikh dobavok k tamponazhnym rastvoram [Research of hydration dynamics and development of expanding additives to oil-well cement]. *Neftianoe khoziaistvo*, 2015, no. 8, pp. 42-44.
15. Chernyshov S.E., Galkin S.V., Krisin N.I., Turbakov M.S., Riabokon E.P. Efficiency improvement of abrasive jet perforation. *In Proceedings of the Society of Petroleum Engineers - SPE Annual Caspian Technical Conference and Exhibition*, Baku, Azerbaijan, 2015. DOI: 10.2118/177375-MS
16. Deng K.H., Zhou N.T., Lin Y.H., Wu Y.X., Chen J. Shu, C., Xie P.F. Failure mechanism and influencing factors of cement sheath integrity under alternating pressure. *Petroleum Science*, 2023. DOI: 10.1016/j.petsci.2023.03.004
17. Li X.R., Gu C.W., Ding Z.C., Feng Y.C. THM coupled analysis of cement sheath integrity considering well loading history. *Petroleum Science*, 2023, vol. 20, pp. 447-459. DOI: 10.1016/j.petsci.2022.09.001
18. Wu Z., Wu G., Xing X., Yang J., Liu S., Xu H., Chang X. Effect of hole on oil well cement and failure mechanism: application for oil and gas wells. *ACS Omega*, 2022, no. 7, pp. 5972-5981. DOI: 10.1021/acsomega.1c06275
19. Fallahzadeh S.H., Shadizadeh S.R., Pourafshary P., Zare M.R. Modeling the perforation stress profile for analyzing hydraulic fracture initiation in a cased hole. *In Proceedings of the Nigeria Annual International Conference and Exhibition*. Tinapa - Calabar, Nigeria, 2010. DOI: 10.2118/136990-MS
20. Xue S., Zhu X., Zhang L., Zhu S., Ye G., Fan X. Research on the Damage of porosity and permeability due to perforation on sandstone in the compaction zone. *CMC*, 2016, vol. 51, no. 1, pp. 21-42. DOI: 10.3970/cmc.2016.051.021
21. Hou B., Cui Z., Ding J.H., Zhang F.S., Zhuang L., Elsworth D. Perforation optimization of layer-penetration fracturing for commingling gas production in coal measure strata. *Petroleum Science*, 2022, vol. 19, pp. 1718-1734. DOI: 10.1016/j.petsci.2022.03.014
22. Li M.H., Zhou F.J., Wang B., Hu X.D., Wang D.B., Zhuang X.Y., Han S.B., Huang G.P. Numerical simulation on the multiple planar fracture propagation with perforation plugging in horizontal wells. *Petroleum Science*, 2022, vol. 19, pp. 2253-2267. DOI: 10.1016/j.petsci.2022.05.004
23. Semenov B.A., Sementsov A.A., Rutskii A.M. Neitralizatsiia fugasnogo deistviia lentochnykh kumuliativnykh perforatorov tipa PKS-80 [Neutralization of the high explosive action of belt cumulative perforators of the PKS-80 type]. *Geofizicheskie metody poiskov i razvedki mestorozhdenii nefti i gaza. Mezhvuzovskii sbornik nauchnykh trudov*. Perm': Permskii gosudarstvennyi universitet, 1996, pp. 82-85.

24. Rastegar R., Munawar M., Nowowiejski D., Granberg S., Cathrine Mehus, Benson A. Mitigating formation damage by using completion with built-in-casing perforations instead of perforation with explosive charges. Society of Petroleum Engineers. *In Proceedings of the SPE European Formation Damage Conference and Exhibition*. Budapest, Hungary, 2015. DOI: 10.2118/174251-MS
25. Savich A.D., El'kind S.Ia. Vtorichnoe vskrytie produktivnykh plastov. Tekhnika i tekhnologii [Secondary opening of productive layers. Equipment and technologies]. *Nauchno-tekhnicheskii vestnik "Karotazhnik"*, 2003, no. 106, pp. 120-134.
26. Krysin N.I., Riabokon' E.P., Turbakov M.S., Chernyshov S.E., Shcherbakov A.A. Sovershenstvovanie ustroistv shchelevoi gidropeskostruinoi perforatsii v neftianykh skvazhinakh [Improvement of devices of abrasive jet perforation in oil wells]. *Neftianoe khoziaistvo*, 2016, no. 8, pp. 129-131.
27. Gaivoronskii I.N., Kostitsyn V.I., Savich A.D., Chernykh I.A., Shumilov A.V. Povyshenie effektivnosti vtorichnogo vskrytiia produktivnykh plastov [Ways of improvement of reservoir completion efficiency]. *Neftianoe khoziaistvo*, 2016, no. 10, pp. 62-65.
28. BVT, available at: https://www.bvt-s.ru/catalog/technological-solution-product/tekhnologiya-perforatsii-na-dinamicheskoy-depresii-dp-deltap/ (accessed 15 December 2023).
29. Parnoe gruppirovanie zariadov v perforatore. Promperforator [Paired grouping of charges in a perforator. Promperforator], available at: http://www.promperforator.ru/catalog/perforating_guns/149060022 (accessed 01 September 2024).
30. Instruktsiia po vskrytiiu plastov streliaiushchimi perforatorami v razvedochnykh obsazhennykh neftegazovykh skvazhinakh [Instructions for opening formations with shooting perforators in exploratory cased oil and gas wells]. Nauchno-proizvodstvennoe ob"edinenie "Soiuzpromgeofizika", Vsesoiuznyi nauchno-issledovatel'skii i proektno-konstruktorskii institut po vzryvnym metodam geofizicheskoi razvedki. Ramenskoe: VNIPIvzryvgeofizika, 1987, 22 p.
31. GOST R 55777-2013. Zariady kumuliativnye. Tekhnicheskie usloviia [GOST R 55777-2013. Cumulative charges. Technical conditions]. Moscow: Standartinform, 2013, 18 p.
32. Seriakov A.V., Podberezhnyi M.Iu., Bocharov O.B., Azamatov O.B. Ustoichivost' zony sochleneniia soosnykh skvazhin razlichnogo diametra (na primere mestorozhdeniia KhMAO) [Junction zone stability in coaxial wells of different diameters (on the example of the Khanty-Mansi Autonomous District oil field)]. *Georesursy*, 2020, vol. 22 (3), pp. 69-78. DOI: 10.18599/grs.2020.3.69-78
33. Chernyshov S.E., Popov S.N., Varushkin S.V., Melekhin A.A., Krivoshchekov S.N., Ren Sh. Nauchnoe obosnovanie metodov vtorichnogo vskrytiia famenskikh otlozhenii iugo-vostoka Permskogo kraia na osnovanii geomekhanicheskogo modelirovaniia [Scientific justification of the perforation methods for Famennian deposits in the Southeast of the Perm region based on geomechanical modelling]. *Zapiski Gornogo instituta*, 2022, vol. 257, no. 5, pp. 732-743. DOI: 10.31897/PMI.2022.51
34. Agzamov F.A., Makhmutov A.N., Tokunova E.F. Issledovanie korrozionnoi stoikosti tamponazhnogo kamnia v magnezial'nykh agressivnykh sredakh [Study of corrosion stability of a cement stone in magnesia aggressive environment]. *Georesursy*, 2019, 21(3), pp. 73-78. DOI: 10.18599/grs.2019.3.73-78
35. Chernikov A.D., Eremin N.A., Stoliarov V.E., Sboev A.G., Semenova-Chashchina O.K., Fitsner L.K. Primenenie metodov iskusstvennogo intellekta dlia vyiavleniia i prognozirovaniia oslozhnenii pri stroitel'stve neftianykh i gazovykh skvazhin: problemy i osnovnye napravleniia resheniia [Application of artificial intelligence methods for identifying and predicting complications in the construction of oil and gas wells: problems and solutions]. *Georesursy*, 2020, vol. 22 (3), pp. 87-96. DOI: 10.18599/grs.2020.3.87-96
36. Popov S.N., Chernyshov S.E., Gladkikh E.A. Vliianie deformatsii terrigennogo kollektora v protsesse snizheniia zaboinogo i plastovogo davleniia na izmenenie pronitsaemosti i produktivnosti skvazhiny [Influence of sandstone reservoir deformations during bottomhole and reservoir pressure decreasing on the permeability and well productivity changes]. *Izvestiia Tomskogo politekhnicheskogo universiteta. Inzhiniring georesursov*, 2022, vol. 333, no. 9, pp. 148-157. DOI: 10.18799/24131830/2022/9/3640
37. Popov S., Chernyshov S., Gladkikh E. Experimental and numerical assessment of the influence of bottomhole pressure drawdown on terrigenous reservoir permeability and well productivity. *Fluid dynamics and materials processing*, 2023, vol. 19, no. 3, pp. 619-634. DOI: 10.32604/fdmp.2022.021936
38. Popov S.N. Opredelenie koeffitsienta zapasa prochnosti tsementnogo kamnia na osnove chislennogo modelirovaniia napriazhenno-deformirovannogo sostoianiia okoloskvazhinnoi zony s uchetom izmeneniia uprugo-prochnostnykh svoistv tsementa v protsesse ego tverdeniia i pod vozdeistviem kislotnogo reagenta [Determination of the safety factor of cement stone based on numerical modeling of the stress-strain state of the near-wellbore zone, taking into account the change in the elastic-strength properties of cement during its hardening and under the influence of an acid reagent]. *SOCAR Proceeding*, 2021, SI no. 2, pp. 8-16. DOI: 10.5510/OGP2021SI200544
39. Popov S.N. Geomekhanicheskoe modelirovanie i analiz ustoichivosti ekspluatatsionnoi kolonny v usloviiakh chastichnogo otsutstviia tsementnogo kamnia [Geomechanical modeling and the casing stability analysis in conditions of cement stone partial absence]. *SOCAR Proceeding*, 2022, SI no. 2, pp. 45-51. DOI: 10.5510/OGP2022SI200726
40. GOST 21153.2-84. Porody gornye. Metody opredeleniia predela prochnosti pri odnoosnom szhatii [GOST 21153.2-84. Rocks. Methods for Determining the Ultimate Strength under Uniaxial Compression]. Moscow: Izdatel'stvo standartov, 1984, 18 p.
41. GOST 28985-91. Porody gornye. Metod opredeleniia deformatsionnykh kharakteristik pri odnoosnom szhatii [GOST 28985-91. Rocks. Method for Determining Deformation Characteristics under Uniaxial Compression]. Moscow: Izdatel'stvo standartov, 1984, 17 p.

Библиографический список

1. Изменение контакта цементного камня с металлом обсадных труб при различных механических воздействиях / Д.А. Крылов, Н.А. Марабаев, Е.Н. Таламанов, В.А. Бурхайло, И.А. Серенко // Бурение. – 1981. – № 7. – С. 18–21.
2. Шишин, К.А. Влияние опрессовки и перфорации скважин на качество разобщения пластов / К.А. Шишин, Т.Ф. Рустамбеков, Д.А. Крылов // РНТС сер. «Бурение». – М.: Изд. ВНИИОЭНГ, 1977. – Вып. 4. – С. 25–27.
3. Оценка сохранности крепи скважин после проведения кумулятивной перфорации с учетом критерия разрушения цементного камня / С.Е. Чернышов, С.Г. Ашихмин, Ю.А. Кашников, А.Д. Савич, А.В. Мосин, А.С. Чухлов // Нефтяное хозяйство. – 2021. – № 6. – С. 50–53. DOI: 10.24887/0028-2448-2021-6-50-53
4. Kremieniewski, M. Recipe of Lightweight Slurry with High Early Strength of the Resultant Cement Sheath / M. Kremieniewski // Energies. – 2020. – Vol. 13. – P. 1583. DOI: 10.3390/en13071583
5. Kremieniewski, M. Hybrid Washer Fluid for Primary Cementing / M. Kremieniewski // Energies. – 2021. – Vol. 14. – P. 1295. DOI: 10.3390/en14051295
6. Comparison of Efficient Ways of Mud Cake Removal from Casing Surface with Traditional and New Agents / M. Kremieniewski, R. Wiśniowski, S. Stryczek, P. Łopata // Energies. – 2021. – Vol. 14. – P. 3653. DOI: 10.3390/en14123653
7. Self-Healing Concrete: Concepts, Energy, Saving and Sustainability / B.A.C. Roque, P.P.F. Brasileiro, Y.B. Brandão, A.A. Casazza, A. Converti, M. Benachour, L.A. Sarubbo // Energies. – 2023. – Vol. 16. – P. 1650. DOI: 10.3390/en16041650
8. Влияние ориентации и схемы размещения каналов щелевой перфорации на проницаемость терригенных коллекторов в околоскважинной зоне пластов / С.Г. Ашихмин, С.Е. Чернышов, Ю.А. Кашников, Д.И.М. Макдоналд // Нефтяное хозяйство. – 2018. – № 6. – С. 132–135. DOI: 10.24887/0028-2448-2018-6-132-135
9. Laboratory investigation on hydraulic fracture propagation in sandstone-mudstone-shale layers / J.C. He, K.S. Zhang, H.B. Liu, M.R. Tang, X.L. Zheng, G.Q. Zhang // Petroleum Science. – 2022. – Vol. 19. – P. 1664–1673. DOI: 10.1016/j.petsci.2022.03.018
10. The role of natural fracture activation in hydraulic fracturing for deep unconventional geo-energy reservoir stimulation / J. Wang, H.P. Xie, S.K. Matthai, J.J. Hu, C.B. Li // Petroleum Science. – 2022. – Vol. 19. – P. 1664–1673. DOI: 10.1016/j.petsci.2023.01.007
11. Influences of Fracturing Fluid Injection on Mechanical Integrity of Cement Sheath under Four Failure Modes / H. Xu, T. Ma, N. Peng, B. Yang // Energies. – 2018. – Vol. 11. – P. 3534. DOI: 10.3390/en11123534
12. Numerical Investigation of Downhole Perforation Pressure for a Deepwater Well / Q. Deng, H. Zhang, J. Li, X. Hou, B. Zhao // Energies. – 2019. – Vol. 12. – P. 3795. DOI: 10.3390/en12193795
13. Study of Downhole Shock Loads for Ultra-Deep Well Perforation and Optimization Measures / Q. Deng, H. Zhang, J. Li, X. Hou, H. Wang // Energies. – 2019. – Vol. 12. – P. 2743. DOI: 10.3390/en12142743
14. Чернышов, С.Е. Исследование динамики гидратации и разработка составов расширяющих добавок к тампонажным растворам / С.Е. Чернышов, А.А. Куницких, М.В. Вотинов // Нефтяное хозяйство. – 2015. – № 8. – С. 42–44.
15. Efficiency improvement of abrasive jet perforation / S.E. Chernyshov, S.V. Galkin, N.I. Krisin, M.S. Turbakov, E.P. Riabokon // In Proceedings of the Society of Petroleum Engineers – SPE Annual Caspian Technical Conference and Exhibition. – Baku, Azerbaijan, 2015. DOI: 10.2118/177375-MS
16. Failure mechanism and influencing factors of cement sheath integrity under alternating pressure / K.H. Deng, N.T. Zhou, Y.H. Lin, Y.X. Wu, J. Chen, C. Shu, P.F. Xie // Petroleum Science. – 2023. DOI: 10.1016/j.petsci.2023.03.004
17. THM coupled analysis of cement sheath integrity considering well loading history / X.R. Li, C.W. Gu, Z.C. Ding, Y.C. Feng // Petroleum Science. – 2023. – Vol. 20. – P. 447–459. DOI: 10.1016/j.petsci.2022.09.001
18. Effect of hole on oil well cement and failure mechanism: application for oil and gas wells / Z. Wu, G. Wu, X. Xing, J. Yang, S. Liu, H. Xu, X. Chang // ACS Omega. – 2022. – No. 7. – P. 5972–5981. DOI: 10.1021/acsomega.1c06275
19. Modeling the perforation stress profile for analyzing hydraulic fracture initiation in a cased hole / S.H. Fallahzadeh, S.R. Shadizadeh, P. Pourafshary, M.R. Zare // In Proceedings of the Nigeria Annual International Conference and Exhibition. – Tinapa – Calabar, Nigeria, 2010. DOI: 10.2118/136990-MS
20. Research on the Damage of porosity and permeability due to perforation on sandstone in the compaction zone / S. Xue, X. Zhu, L. Zhang, S. Zhu, G. Ye, X. Fan // CMC. – 2016. – Vol. 51, no. 1. – P. 21–42. DOI: 10.3970/cmc.2016.051.021
21. Perforation optimization of layer-penetration fracturing for commingling gas production in coal measure strata / B. Hou, Z. Cui, J.H. Ding, F.S. Zhang, L. Zhuang, D. Elsworth // Petroleum Science. – 2022. – Vol. 19. – P. 1718–1734. DOI: 10.1016/j.petsci.2022.03.014
22. Numerical simulation on the multiple planar fracture propagation with perforation plugging in horizontal wells / M.H. Li, F.J. Zhou, B. Wang, X.D. Hu, D.B. Wang, X.Y. Zhuang, S.B. Han, G.P. Huang // Petroleum Science. – 2022. – Vol. 19. – P. 2253–2267. DOI: 10.1016/j.petsci.2022.05.004
23. Семенов, Б.А. Нейтрализация фугасного действия ленточных кумулятивных перфораторов типа ПКС-80 / Б.А. Семенов, А.А. Семенцов, А.М. Руцкий // Геофизические методы поисков и разведки месторождений нефти и газа: Межвуз. сб. науч. тр. – Пермь: ПГУ, 1996. – С. 82–85.
24. Mitigating formation damage by using completion with built-in-casing perforations instead of perforation with explosive charges. Society of Petroleum Engineers / R. Rastegar, M. Munawar, D. Nowowiejski, S. Granberg, Mehus Cathrine, A. Benson // In Proceedings of the SPE European Formation Damage Conference and Exhibition. – Budapest, Hungary, 2015. DOI: 10.2118/174251-MS

25. Савич, А.Д. Вторичное вскрытие продуктивных пластов. Техника и технологии / А.Д. Савич, С.Я. Элькинд // НТВ «Каротажник». – 2003. – № 106. – С. 120–134.
26. Совершенствование устройств щелевой гидропескоструйной перфорации в нефтяных скважинах / Н.И. Крысин, Е.П. Рябоконь, М.С. Турбаков, С.Е. Чернышов, А.А. Щербаков // Нефтяное хозяйство. – 2016. – № 8. – С. 129–131.
27. Повышение эффективности вторичного вскрытия продуктивных пластов / И.Н. Гайворонский, В.И. Костицын, А.Д. Савич, И.А. Черных, А.В. Шумилов // Нефтяное хозяйство. – 2016. – № 10. – С. 62–65.
28. BVT [Электронный ресурс]. – URL: https://www.bvt-s.ru/catalog/technological-solution-product/tekhnologiya-perforatsii-na-dinamicheskoy-depresii-dp-deltap/ (дата обращения: 15.12.2023).
29. Парное группирование зарядов в перфораторе. Промперфоратор [Электронный ресурс]. – URL: http://www.promperforator.ru/catalog/perforating_guns/149060022 (дата обращения: 01.09.2024).
30. Инструкция по вскрытию пластов стреляющими перфораторами в разведочных обсаженных нефтегазовых скважинах / НПО «Союзпромгеофизика», Всесоюз. н.-и. и проект.-конструкт. ин-т по взрывным методам геофиз. разведки. – Раменское : ВНИПИвзрывгеофизика, 1987. – 22 с.
31. ГОСТ Р 55777–2013. Заряды кумулятивные. Технические условия. – М.: Стандартинформ, 2013. – 18 с.
32. Устойчивость зоны сочленения соосных скважин различного диаметра (на примере месторождения ХМАО) / А.В. Серяков, М.Ю. Подбережный, О.Б. Бочаров, О.Б. Азаматов // Георесурсы. – 2020. – Т. 22(3). – С. 69–78. DOI: 10.18599/grs.2020.3.69-78
33. Научное обоснование методов вторичного вскрытия фаменских отложений юго-востока Пермского края на основании геомеханического моделирования / С.Е. Чернышов, С.Н. Попов, С.В. Варушкин, А.А. Мелехин, С.Н. Кривощеков, Ш. Рен // Записки Горного института. – 2022. – Т. 257, № 5. – С. 732–743. DOI: 10.31897/PMI.2022.51
34. Агзамов, Ф.А. Исследование коррозионной стойкости тампонажного камня в магнезиальных агрессивных средах / Ф.А. Агзамов, А.Н. Махмутов, Э.Ф. Токунова // Георесурсы. – 2019. – 21(3). – С. 73–78. DOI: 10.18599/grs.2019.3.73-78
35. Применение методов искусственного интеллекта для выявления и прогнозирования осложнений при строительстве нефтяных и газовых скважин: проблемы и основные направления решения / А.Д. Черников, Н.А. Еремин, В.Е. Столяров, А.Г. Сбоев, О.К. Семенова-Чащина, Л.К. Фицнер // Георесурсы. – 2020. – Т. 22(3). – С. 87–96. DOI: 10.18599/grs.2020.3.87-96
36. Попов, С.Н. Влияние деформаций терригенного коллектора в процессе снижения забойного и пластового давления на изменение проницаемости и продуктивности скважины / С.Н. Попов, С.Е. Чернышов, Е.А. Гладких // Известия Томского политехнического университета. Инжиниринг георесурсов. – 2022. – Т. 333, № 9. – С. 148–157. DOI: 10.18799/24131830/2022/9/3640
37. Popov, S. Experimental and numerical assessment of the influence of bottomhole pressure drawdown on terrigenous reservoir permeability and well productivity / S. Popov, S. Chernyshov, E. Gladkikh // Fluid dynamics and materials processing. – 2023. – Vol. 19, no. 3. – P. 619–634. DOI: 10.32604/fdmp.2022.021936
38. Попов, С.Н. Определение коэффициента запаса прочности цементного камня на основе численного моделирования напряженно-деформированного состояния околоскважинной зоны с учетом изменения упруго-прочностных свойств цемента в процессе его твердения и под воздействием кислотного реагента / С.Н. Попов // SOCAR Proceeding. – 2021. – SI № 2. – С. 8–16. DOI: 10.5510/OGP2021SI200544
39. Попов, С.Н. Геомеханическое моделирование и анализ устойчивости эксплуатационной колонны в условиях частичного отсутствия цементного камня / С.Н. Попов // SOCAR Proceeding. – 2022. – SI № 2. С. 45–51. DOI: 10.5510/OGP2022SI200726
40. ГОСТ 21153.2–84. Породы горные. Методы определения предела прочности при одноосном сжатии. – М.: Издательство стандартов, 1984. – 18 с.
41. ГОСТ 28985–91. Породы горные. Метод определения деформационных характеристик при одноосном сжатии. – М.: Издательство стандартов, 1984. – 17 с.

Funding. The research was supported by the Ministry of Science and Higher Education of the Russian Federation (project No. FSNM-2024-0005).

Conflict of interest. The authors declare no conflict of interest.

The authors' contribution is equal.